Vibrational Relaxation of CN Stretch of Pseudo-Halide Anions (OCN^-, SCN^-, and $SeCN^-$) in Polar Solvents†

Victor Lenchenkov, Chunxing She, and Tianquan Lian*

Department of Chemistry, Emory University, Atlanta, Georgia 30322

Received: April 14, 2006; In Final Form: June 9, 2006

The vibrational relaxation dynamics of pseudo-halide anions XCN^- (X=O, S, Se) in polar solvents were studied to understand the effect of charge on solute-to-solvent intermolecular energy transfer (IET) and solvent assisted intramolecular vibrational relaxation (IVR) pathways. The T_1 relaxation times of the CN stretch in these anions were measured by IR pump/IR probe spectroscopy, in which the 0−1 transition was excited, and the 0−1 and 1−2 transitions were monitored to follow the recovery of the ground state and decay of the excited state. For these anions in five solvents, H_2O, D_2O, CH_3OH, CH_3CN, and $(CH_3)_2SO$, relaxation rates followed the trend of $OCN^- > SCN^- > SeCN^-$. For these anions and isotopes of SCN^-, the relaxation rate was a factor of a few (2.5−10) higher in H_2O than in D_2O. To further probe the solvent isotope effect, the relaxation rates of $S^{12}C^{14}N^-$, $S^{13}C^{14}N^-$, and $S^{12}C^{15}N^-$ in deuterated methanols (CH_3OH, CH_3OD, CH_3OH, CD_3OD) were compared. Relaxation rate was found to be affected by the change of solvent vibrational band at the CN^- stretching mode (CD_3 symmetric stretch) and lower frequency regions, suggesting the presence of both direct IET and solvent assisted IVR relaxation pathways. The possible relaxation pathways and mechanisms for the observed trends in solute and solvent dependence were discussed.

Introduction

Because of its essential role in chemical reaction dynamics, molecular vibrational energy relaxation in the condensed phase continues to draw intense theoretical and experimental interest.[1−9] It was observed in recent years that vibrational relaxation dynamics of polar diatomic molecules (such as I_2^- [10,11] and HgI[12,13]) was orders of magnitude faster than their nonpolar counterparts (such as I_2[4]) of similar low oscillator frequency. Ultrafast vibrational relaxation in the 10s ps time scale was also observed for the high-frequency vibrational mode of CN^- in water.[14,15] MD simulations has revealed that fast relaxation dynamics of polar molecules in polar solvent could be attributed to the presence of Coulomb interactions[16−18] and charge fluctuation of the solute.[10,19] The mechanism by which the slowly varying Coulomb forces facilitate relaxation of high frequency vibration has been carefully examined recently.[12,20] It is understood now that the Coulomb forces bring the solute and solvent molecules closer, which enhances the relaxation caused by the repulsive interactions.

The mechanisms of vibrational relaxation of charged polyatomic solutes in polar solvents are less well understood. For neutral polyatomic molecules in solution, the relaxation of a high-frequency mode is often found to proceed through solvent assisted intramolecular vibrational relaxation (IVR), with the solvent providing low-frequency modes to fill the energy gap between solute intramolecular states.[5,7,9,21−26] Can the coulomb forces and fluctuating charge enhance the rate of direct solute−solvent relaxation to the extent that it becomes a competitive pathway? There have been a few reports of vibrational relaxation of high-frequency modes in charged triatomic molecules, such as the CN stretch modes of OCN^- and SCN^- [27,28] and asymmetric stretching mode of N_3^-.[27,29−31] Among these, vibrational relaxation dynamics of N_3^- has been most extensively studied.[19,27,29−33] For N_3^- in water, the T_1 population relaxation time for the asymmetric mode was found to be 1.2 ps.[27] MD simulation suggests that the relaxation occurred by both the direct energy transfer to solvent and solvent assisted IVR pathways, and the relaxation rate is enhanced in this system because of the intramolecular charge fluctuation.[19] An order of magnitude slower relaxation time was observed for N_3^- in an aprotic solvent.[27] The relaxation time is also considerably faster than the CN stretching mode of SCN^- in similar solvents, despite similar vibrational frequency. It remains unclear how the relaxation dynamics depends on the properties of solute and solvent molecules. A more systematic study of the solute and solvent dependence may provide some insight on the competing IVR and direct solute−solvent relaxation pathways.

Pseudo-halide anions, XCN^- (where X is O, S, or Se) may serve as ideal candidates for a systematic experimental and theoretical examination of vibrational relaxation dynamics in polar polyatomic molecules. These linear anions have only three normal modes, v_1, v_2 (doubly degenerate), and v_3, which are both IR and Raman active, as shown in Table 1. They are also commonly labeled as CX stretch, bending, and CN stretch modes, respectively. In SCN^- and $SeCN^-$, the v_1 and v_3 modes are dominated by localized motion of CX and CN bond vibrations, but in OCN^-, these modes do not localize on these bonds.[34] Going from O, S to Se, the frequency of CX stretch and the bending modes decreases, and the partial charges on the X(−), C(+), and N(−) atoms become smaller. The latter was inferred from the decreasing interaction (hydrogen bonding and counterion pairing) with solvents and verified by ab initio calculations.[34−36]

In this work, we report a comprehensive experimental study of the vibrational relaxation dynamics of these anions and their selected isotopes in polar solvents. We measured the T_1 relaxation time of CN stretch mode by femtosecond time-

† Part of the special issue "Charles B. Harris Festschrift".

* To whom correspondence should be addressed. E-mail: tlian@emory.edu.

10.1021/jp062326l CCC: $33.50
Published on Web 07/29/2006

TABLE 1: Fundamental Frequencies of Normal Modes of XCN^- Anions[37−39]

	ν_1 or ν_{CX} cm^{-1}	ν_2 or ν_{bend} cm^{-1}	ν_3 or ν_{CN} (cm^{-1})/ molar abs in H_2O $(Mcm)^{-1}$	spectral activity
OCN^-	1310 (1313)	632 (637)*	2168/∼1800	IR, Raman
SCN^-	743	470	2063/∼500	IR, Raman
$SeCN^-$	560	420	2073/∼1200	IR, Raman

resolved mid-infrared pump−probe spectroscopy. The relaxation times of XCN^- (X = O, S, Se) in five solvents, H_2O, D_2O, CH_3OH, CH_3CN, and $(CH_3)_2SO$, were measured to allow the comparison of the relaxation rates of different anions in the same solvent and the same anions in different solvents. To help understand the solvent and solute dependence, we also studied the solvent isotope effects in H_2O and D_2O and in deuterated methanols for these anions and two isotopes of SCN^- ($S^{13}C^{14}N^-$ and $S^{12}C^{15}N^-$). The possible pathways of the relaxation processes and mechanism for the observed trends in relaxation rates in different anions are discussed.

Experimental Setup

The femtosecond mid-infrared pump−probe spectrometer was based on a 1 kHz Ti:sapphire regenerative amplifier (CPA-1000, Clark-MXR) which was seeded with single mode Ti:sapphire oscillator (Vitesse, Coherent). The regenerative amplifier produced pulses of ∼120 fs duration at ∼804 nm with ∼900 μJ/pulse. The 500 μJ/pulses of the fundamental were used to pump an optical parametric amplifier to generate two near-infrared pulses at about 1.5 and 1.9 μm, respectively. These two pulses were then mixed in a $AgGaS_2$ crystal to generate mid-infrared light at about 5 μm wavelength with ∼1.5 μJ/pulse energy and ∼200 cm^{-1} fwhm.

The mid-infrared beam was split by a beam splitter (9:1 ratio) to produce pump and probe pulses. The pump beam went through a variable translation stage to change pump−probe delay time. After the translation stage, the pump beam was chopped by an optical chopper at 500 Hz frequency. Then signal, idler, and their visible harmonics (generated in $AgGaS_2$) were reflected by a Ge window into a photodiode which was used to correlate probe transmittance with blocked and unblocked mid-infrared pump beam. In both the pump and the probe arms, the residual signal and idler pulses were filtered out with long-pass filters. A He−Ne laser was used to trace pump and probe paths to ensure their spatial overlap in the sample. The mid-infrared probe pulse was spectrally dispersed in an imaging spectrograph (CVI Digikrom 240) and imaged onto a 32 element HgCdTe-(MCT) array detector. The amplified outputs of the 32 elements were measured for every laser shot at a 1 kHz repetition rate. All spectra were recorded with a spectral resolution of 2.5 cm^{-1}/element. To minimize low frequency laser fluctuations every other pump pulse was blocked with a synchronized chopper (New Focus model 3500) at 500 Hz, and the absorbance change was calculated with two adjacent probe pulses (pump blocked and pump unblocked). Transient kinetics at 32 wavelengths was simultaneously collected, from which transient spectra at different delay times were constructed.

The zero delay time and instrument response for a mid-IR pump−probe experiment were determined from a coherent spike around time zero for each sample. The typical instrument response, which was determined in every experiment, could be well represented by a Gaussian function with fwhm ≈ 300 fs. The diameters of the pump and probe beams were ∼200 μm. The pump−probe relative polarization was controlled by MgF_2 wave-plate (Alphalas GmbH) which was set in the pump arm. For population relaxation time (T_1) measurements, the pump−probe relative polarization was set at the magic angle (54.7 degrees). To extract anisotropy dynamics, the relaxation dynamics were measured at both parallel and perpendicular pump−probe relative polarization by changing the pump polarization. To minimize effect of laser intensity fluctuations on anisotropy dynamics, the pump polarizations were alternating in the series of back-to-back scans. After collecting these scans, they were averaged separately to obtain averaged dynamics for each relative polarization.

The pump and probe mid-infrared beams were focused at sample solutions in a 56 μm thick static cell (thickness determined by Teflon spacer) with a 2 in. diameter off-axis parabolic mirror. Fresh 0.1−0.2 M sample solutions of XCN^- anions were prepared with NaOCN (Aldrich 99.9%), $NaS^{12}C^{14}N$ (J. T. Baker 99.6%), $KS^{13}C^{14}N$ (Icon Service 99%), $KS^{12}C^{15}N$ (Icon Service 99%), and KSeCN (Aldrich 99%) salts. Since NaOCN is not soluble in acetonitrile, the $N(C_4H_9)_4OCN$ (Fluka) has been used instead. In the case of OCN^- solutions, only freshly prepared solutions were studied since there were indications that OCN^- could substantially degrade at ambient conditions within 2−3 days.[37] Aqueous solutions were prepared with H_2O purified with Barnstead NANOpure II system (water resistivity after purification ≈ 17.5 MΩ-cm). Other solvents, D_2O (Aldrich 99.9 at. % D), CH_3OH (Aldrich 99.8%), CH_3OD (Aldrich 99%), CD_3OH (Aldrich 99%), CD_3OD (Aldrich 99%), CH_3CN (Fisher Chemicals 99.9%), and $(CH_3)_2SO$ (Fisher Chemicals 99.9%) were used as received. Samples were routinely checked for degradation by taking their FTIR spectra with a Nicolet Instruments FTIR spectrometer. The samples did not show any evidence of degradation after their exposure to mid-infrared beams. IR spectra of pure solvents were also measured with the FTIR spectrometer.

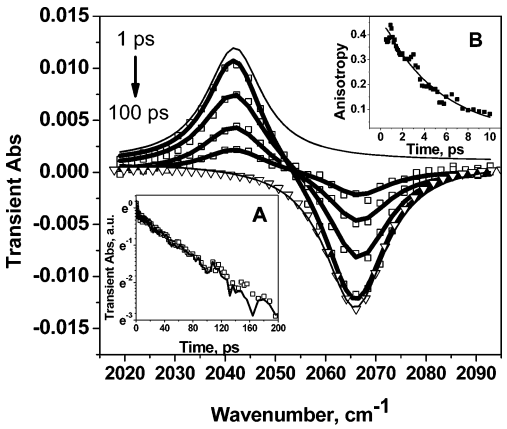

Figure 1. Selected transient spectra (symbols) and their fits (solid thick lines) of the CN stretch of 0.1 M KSeCN in CH_3CN at 1, 20, 50, and 100 ps delay times collected with pump-probe relative polarization at the magic angle. The fit consists of two Lorentzians (thin lines shown for transient spectrum collected at 1 ps delay time): the negative higher frequency band is assigned to the 0−1 (bleach) band and the positive lower frequency one is ascribed as the 1−2 (adsorption) band. The centers and widths of the 0−1 and 1−2 bands were fixed at all delay times during the fitting, while amplitudes of the bands were optimized. The FTIR spectrum of the 0−1 CN stretch band is shown by open triangles. Shown in the inset is (A) the normalized amplitude dynamics of 0−1 (solid line) and 1−2 band (open squares) of the CN stretch of $SeCN^-$ in CH_3CN obtained with spectral fitting and (B) the typical anisotropy dynamics (symbols) and its fit (solid lines) shown for 0.1 M KeSeCN in CH_3CN. The anisotropy was calculated from the amplitude dynamics of the 0−1 band which was determined by fitting the transient spectra measured at parallel and perpendicular pump−probe relative polarization.

TABLE 2: Fitting Results of CN Stretch Relaxation Dynamics of XCN^- [X = O, S, Se] in Polar Solvents

anion	solvent	ν_{CN} (0−1)/ anharmonicity shift cm^{-1}	Fwhm 0−1/1−2 bands cm^{-1}	T_1 0−1/1−2 bands ps	T_R 0−1/1−2 bands ps
			H_2O		
OCN^-	(3.31)[a]	2168/18	26/55	0.71[b]/0.9	∼1[b]
$S^{12}C^{14}N^-$	(3.16)	2064/27	32/37	2.7[b]/2.7	3
$S^{13}C^{14}N^-$	(2.68)	2017/28	25/36	2.8/2.9	
$S^{12}C^{15}N^-$	(2.91)	2038/25	32/35	2.8/3.1	
$SeCN^-$	(3.24)	2074/25	41/37	3.8/3.8	2.3
			D_2O		
OCN^-	(2.96.)	2160/20	17/26	2.3/2.3	2.5
$S^{12}C^{14}N^-$	(1.03)	2063/27	35/34	21.1[b]/22.0	4.5[b]
$S^{13}C^{14}N^-$	(0.67)	2015/28	33/32	16.2/17.0	
$S^{12}C^{15}N^-$	(0.81)	2037/23	34/36	24.9/25.2	
$SeCN^-$	(1.17)	2076/23	47/38	38.2/39.4	4.0/3.5
OCN^-		2162/19	22/22	5.0/5.6	6[b]/8.7
			CH_3OH[c]		
$S^{12}C^{14}N^-$		2057/34	58/30	19.7/20.7[c]	6.2/4.4[c]
$SeCN^-$		2071/36	47/30	39.6/39.8	8.2/8.2
OCN^-		2147/22	21/25	3.6/3.6	1.6/1.8
			$(CH_3)_2SO$		
$S^{12}C^{14}N^-$		2055/25	14/16	24.5/24.1	8.5/6
$SeCN^-$		2064/23	13/13	112/118	5/3
OCN^-		2140, 2150/23.5[d]	11, 14/11, 14	23, 3.9/17, 3.6	1, 11.4/2.4, 10
			CH_3CN		
$S^{12}C^{14}N^-$		2059/23	18/20	35.0/35.0	1.6,60/1.5,71[e]
$SeCN^-$		2067/24	13/13	62.0/69.0	5.2/6.3

[a] The solvent molar absorptions $(Mcm)^{-1}$ which are measured at the peak of 0−1 band of CN stretch of the XCN^- are taken from Bertie et al.[41] [b] These fitting results are in good agreement with previously reported ones by Li et al.[27] and Zhong et al.[28] [c] Li et al.[27] report T_1= 11 and T_R= 8.7 ps for 0.3−0.5 M KSCN in methanol solutions. [d] In the case of OCN^- in CH_3CN, both 0−1 and 1−2 CN stretch bands have two peaks. Fitted as Lorentzians, the peaks of the 0−1 band (FTIR spectrum) are centered at 2140 and 2150 cm^{-1} with fwhm 11 and 14 cm^{-1}, respectively. To fit transient spectra, the widths of the peaks of the 1−2 band were assumed to be the same as the ones of 0−1 band. It was also assumed that anharmonicity shifts for both peaks of the CN stretch are the same. The amplitude dynamics of the peaks was determined by transient spectral fitting at each delay time. During spectral fitting the centers and the widths of the peaks in both 0−1 and 1−2 bands were kept fixed. [e] Anisotropy dynamics of SCN^- in CH_3CN is characterized by two exponential decay.

Results

1. Measurements of Population Relaxation Time, T_1, of CN Stretch. The typical transient difference absorption spectra of XCN^-, measured after excitation at the 0−1 transition of CN stretching mode, consist of two bands: a decrease in absorption (bleach) at 0−1 band caused by vibrational depopulation of CN stretch at the ground state and an increase in absorption at the red-shifted 1−2 band assigned to population change at $v = 1$. Depending on the anion, the transient signal levels at the maximum of the band(s) were in the range of 10−50 mOD for 0.1−0.2 M solutions, with a negligible (<0.5 mOD) contribution from samples containing only the neat solvent. An example of the transient spectra for $SeCN^-$ in CH_3CN is shown in Figure 1. The frequency difference between the centers of the 0−1 and 1−2 bands is attributed to the anharmonicity of the CN stretch mode.

The transient spectra for most of the samples (except methanol solutions) show a well-defined isobestic point. In general, both the 0−1 and 1−2 bands can be adequately described by a Lorentzian function. However, it does not indicate a homogeneously broadened line shape. For example, in the case of SCN^- in CH_3OH, the FTIR spectrum of 0−1 band consisted of at least four components, which were previously assigned by Bachelin et al.[40] and Schultz et al.[34,36] to different hydrogen-bonded solute−solvent species. The resolution and signal-to-noise ratio of our time-resolved spectrometer (∼2.3 cm^{-1}) is not high enough to clearly resolve these subtle features. Therefore, to simplify transient spectra fitting, we fit it by a single line shape function, which happens to be adequately described by a Lorentzian.

The transient spectra of CN stretch of XCN^- at each delay time were well fitted as a sum of two Lorentzians (0−1 and 1−2 bands respectively) and an offset constant (to account for small baseline shifts). The widths and centers of 0−1 bands in the transient spectra of the samples were fixed to the values determined from corresponding FTIR spectra. These parameters are in good agreement with previously reported ones.[27,28,34−36] The centers and widths of the 1−2 bands were found iteratively and also kept fixed for all delay times. Therefore, only amplitudes of the Lorentzians were optimized at each delay time during the spectral fitting. The parameters for these fits are summarized in Table 2.

We verified that for most samples, the quality of the fits with fixed values of the centers and widths of the 1−2 bands were not significantly different from fits where these parameters were variable. The only exception is found for methanol solutions of XCN^-, in which the quality of the fits can be slightly improved by optimizing peak positions because of the small blue shifts (∼3 cm^{-1}) of the bands during the first ∼3 ps.

The peak positions and anharmonic shifts for these pseudohalide anions in different solvents agree well with previously reported values.[27,28] The anharmonic shift has typical values in the range of 20 to 30 cm^{-1} with the highest values for SCN^- and $SeCN^-$ in methanol (∼36 and 34 cm^{-1}, respectively) and the lowest values for OCN^- in water and methanol (18 and 19 cm^{-1}, respectively). The amplitudes of the 0−1 and 1−2 bands obtained from the spectral fitting show the same kinetics. For all systems, the amplitude dynamics of these bands can be adequately described by single-exponential decay (see for example Figures 2 and 4). The time constant of exponential

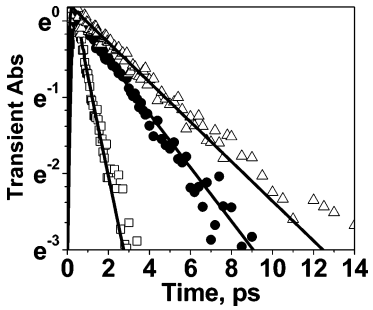

Figure 2. The relaxation dynamics of the CN stretch of OCN^- (open squares), SCN^- (solid circles), and $SeCN^-$ (triangles) in H_2O and their fits (solid lines).

decay is assigned to the population relaxation time of CN stretch, T_1, and is listed in Table 2.

The same procedure was also used to fit transient absorption spectra measured at perpendicular and parallel pump−probe relative polarization. The resulting time dependent amplitudes were used to calculate the anisotropy dynamics according to eq 1

$$a(t) = \frac{A(t)_{||} - A(t)_{\perp}}{A(t)_{||} + 2A(t)_{\perp}} \quad (1)$$

where $A(t)_{||}$ and $A(t)_{\perp}$ are the fitted amplitudes for parallel and perpendicular relative polarization. In all cases, except for OCN^- in CH_3CN, the 0−1 and 1−2 bands give the same anisotropy decay dynamics and can be well fit by single-exponential decay. A typical example of the anisotropy dynamics and its fit are shown in inset B of Figure 1 for $SeCN^-$ in CH_3CN. For OCN^- in CH_3CN, the anisotropy decay is described by a double-exponential function. Since anisotropy decay is attributed to orientational relaxation of the solute molecule, the decay time constant, listed in Table 2, is a measure of the reorientation time, T_R.

It has been reported that at high concentration, pairing of the counterion with anion is significant[42] and affects the vibration population and orientational relaxation dynamics.[14,30] This may lead to a T_1 relaxation time that is dependent on solute concentration and dielectric strength of the solvent. The effects of solute concentration and ionic strength were checked for SCN^- by comparing dynamics of CN stretch relaxation in 0.2 M NaSCN in D_2O, 2 M NaSCN in D_2O, and 0.2 M NaSCN with 2 M $MgSO_4$ in D_2O. SCN^- was chosen for this purpose because it has the lowest CN stretch molar absorption among investigated anions (which allowed us to investigate a wider range of concentrations than if we had chosen OCN^- or $SeCN^-$). It was found that vibrational relaxation rates of CN stretch of SCN^- in all three aforementioned solutions were the same. As it was mentioned above, the vibrational relaxation dynamics for investigated anions listed in Table 2 was measured for 0.1−0.2 M solutions. For SCN^- in H_2O and D_2O, the effect of the ion pair is negligible. However, the stability of the ion pair increases when solvent dielectric decreases. Ion pair formation has been known to affect the CN stretching mode frequency in these pseudo-halide anions.[34,42] The FTIR spectra of the samples studied did not show peaks that were attributable to ion pairs,[34] except for OCN^- in CH_3CN. In the latter case, there were two distinct peaks at 2140 and 2150 cm^{-1} respectively, whose origins remain unclear. Thus, based on these observations, we assume that the vibrational relaxation time of the investigated anions listed in Table 2, with the exception of OCN^- in CH_3CN, is attributable to free anions in solution.

2. Anion and Solvent Dependence. The relaxation rates among investigated solutes in the same solvent are found to be quite different, as shown in Table 2. Shown in Figure 2 is a comparison of the CN stretching mode relaxation dynamics of OCN^-, SCN^-, and $SeCN^-$ in H_2O. The dynamics is the fastest for OCN^- and the slowest for $SeCN^-$ in water. The same trend is observed in all other solvents investigated so far, which include D_2O, CH_3OH, CH_3CN, and $(CH_3)_2SO$. The relaxation dynamics of XCN^- in last four solvents are shown in Figure 3.

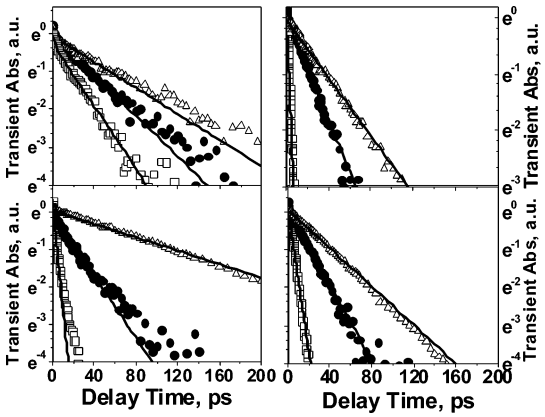

Figure 3. CN stretch vibrational relaxation dynamics of 0.1 M NaOCN (open squares), NaSCN (solid circles), and KSeCN (open triangles) in CH_3CN (top left panel), $(CH_3)_2SO$ (bottom left panel), D_2O (top right panel), and CH_3OH (bottom right panel).

The vibrational relaxation dynamics of CN stretch of each investigated anion also varies with solvent. In light of the important role of Coulomb interaction in the vibrational relaxation of diatomic molecules, such as CN^-,[15] we have compared vibrational relaxation in solvents with different dipole moments. However, the observed vibrational relaxation dynamics is substantially slower for all investigated pseudo-halides in the solvents with larger electrostatic dipole moments (such as acetonitrile and DMSO) than in those with significantly smaller dipole moments (such as water and methanol). In fact, the measured relaxation rate decreases in the series $H_2O > D_2O > CH_3OH > CH_3CN$, DMSO (the relaxation dynamics of OCN^- and SCN^- is slower in CH_3CN than in DMSO while in the case of $SeCN^-$, the relaxation dynamics is slower in DMSO than in CH_3CN, see Table 2).

The reorientation times, T_R, which were determined from the anisotropy dynamics, do not indicate any obvious trend among anions in any given solvent. In the group of the investigated solvents, the reorientation times of the XCN^- in aqueous solutions are generally faster than ones measured in CH_3OH, DMSO, and CH_3CN solutions.

3. Solute and Solvent Isotope Effect. For diatomic solute molecules, the direct energy transfer to solvent is the only way to dispose vibrational energy. Hamm et al.[15] have shown that the CN^- vibrational relaxation rate clearly correlates with IR molar absorption of water. To investigate whether there exists a similar correlation for XCN^- anions, the vibrational relaxation rates of CN stretch were measured for three isotope labeled thiocyanate anions $S^{12}C^{14}N^-$, $S^{12}C^{15}N^-$, and $S^{13}C^{14}N^-$ in H_2O and D_2O and CH_3OH, CH_3OD, CD_3OH, and CD_3OD. The CN stretch frequencies of these thiocyanate anions are listed in Tables 2 and 3).

The vibrational relaxation dynamics for each of the three isotope labeled thiocyanates are faster in H_2O than in D_2O. However, they do not demonstrate clear correlation with solvent molar absorption (measured at the peak of the 0−1 band of CN stretch). In a previous study of several isotope substituted cyanides in H_2O and D_2O, the T_1 relaxation time of the CN stretching mode was found to correlate with solvent molar

TABLE 3: CN Stretch Relaxation Dynamics of Isotope Labeled Thiocyanates in Methanol

anion	ν_{CN} (0−1)/fwhm[a] cm^{-1}	T_1[b] ps CH_3OH	CH_3OD	CD_3OH	CD_3OD
$S^{12}C^{14}N^-$	2057/58	20.4	14	5.7	5.6
$S^{12}C^{15}N^-$	2037/57	18.7	13.6	10.7	8.2
$S^{13}C^{14}N^-$	2015/58	24.7	13.7	18.6	11.7

[a] Shown centers and widths of 0−1 CN stretch bands were determined from FTIR spectra of anions in CH_3OH. For each isotope labeled anion, the center and width are practically the same in all methanol solutions. [b] The CN stretch relaxation rates of the samples were determined by fitting measured transient dynamics at the maximum of the 1−2 band.

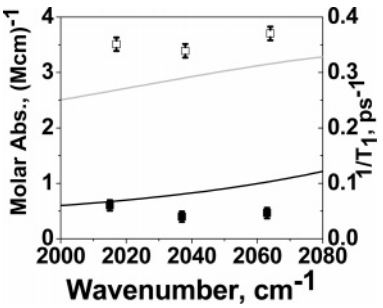

Figure 4. Left vertical axis is the IR molar absorption of H_2O (gray line) and D_2O (black line) in the region of the CN stretch frequencies of $S^{12}C^{14}N^-$ (2064 cm^{-1}), $S^{12}C^{15}N^-$ (2038 cm^{-1}), and $S^{13}C^{14}N^-$ (2017 cm^{-1}). Right vertical axis is the vibrational relaxation rate $1/T_1$ of the CN stretch of the aforementioned isotope labeled thiocyanate anions (see also Table 2) in H_2O (squares) and in D_2O (triangles).

absorptivity.[15] The products of T_1 time and solvent molar absorptivity were found to be practically the same for all isotope labeled cyanides, suggesting a strong dependence of relaxation rate on the solvent spectral density in the direct solute-to-solvent vibrational energy transfer process. The similar products calculated in this work for isotope labeled thiocyantes in aqueous solutions are quite different in D_2O and H_2O. The ratio of relaxation rates for these SCN^- molecules in H_2O and D_2O are larger than the ratio of solvent molar absorptivities measured at frequencies of the 0−1 CN stretch band of corresponding anions in each solvent, see Figure 4 (molar absorption values are shown in brackets in the solvent column of Table 2).

Because of the broad and overlapped bands of water IR spectra and relatively narrow range of CN stretch frequencies covered by the isotopes studied here, a conclusive identification of the role of the direct solute-to-solvent vibrational relaxation pathway is difficult. To further investigate the presence of this relaxation pathway, we compared the vibrational relaxation rate of the CN stretch mode in a series of isotope labeled thiocyantes, $S^{12}C^{14}N^-$, $SC^{15}N^-$, $S^{13}CN^-$, in CH_3OH, CH_3OD, CD_3OH, and CD_3OD. Within the spectral window of solute CN stretch mode, there is large difference in the solvent spectra, as shown in Figure 6. As in the case of aqueous solutions, the center and the width of CN stretch band of each isotope labeled thiocyanate are similar in all four methanol solutions. However the relaxation dynamics of CN stretch of these samples is quite different (see Figure 5 and Table 3).

The population relaxation time, T_1, decreases in the series: $CH_3OH < CH_3OD < CD_3OH < CD_3OD$ (except $S^{13}C^{14}N^-$ in CD_3OH). The substitution of the methyl hydrogen by deuterium increases CN stretch relaxation rates, but this effect is dependent on solute frequency. The increase in relaxation rate from CH_3OH to CD_3OH is small (< ∼25%) in $S^{13}C^{14}N^-$(at 2015 cm^{-1}) and is much larger (∼ 4-fold) in $S^{12}C^{14}N^-$ (at 2057 cm^{-1}). The

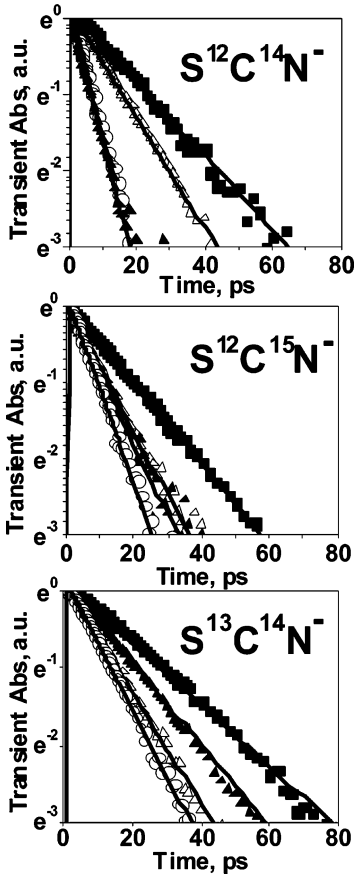

Figure 5. CN stretch relaxation dynamics of CN stretch of $S^{12}C^{14}N^-$ (2057 cm^{-1}), $S^{12}C^{15}N^-$ (2038 cm^{-1}), and $S^{13}C^{14}N^-$ (2017 cm^{-1}) in CH_3OH (solid squares), CH_3OD (open triangles), CD_3OH (solid triangles), and CD_3OD (open circles).

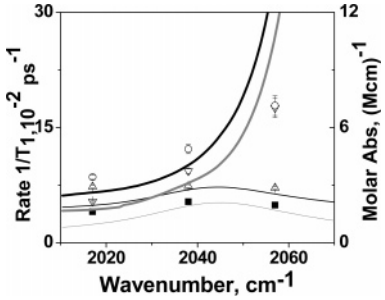

Figure 6. The correlation between relaxation rates $1/T_1$ of SCN^- isotopes (symbols) and molar absorption coefficient of the solvents (lines) in CH_3OH (square, thin gray line), CH_3OD (triangle, thin black line), CD_3OH (inverse triangle, thick gray line), and CD_3OD (circles, thick black line).

relaxation rates show a clear increase with increasing CN stretch frequency in both CD_3OH and CD_3OD, as shown in Figure 6. A similar trend is not present in CH_3OH and CH_3OD. An examination of the IR spectra of these solvents reveals the presence of the strong band at ∼2070 cm^{-1} in CD_3OH and CD_3OD, which have been assigned to CD_3 symmetric stretching mode.[43] The relaxation rates of thiocyanate anions in CD_3OH and CD_3OD appear to correlate with the IR absorption of CD_3 stretching band in these solvents, as shown in Figure 6. This correlation indicates the presence of direct solute-to-solvent vibrational relaxation of CN stretch of SCN^- to the CD_3 symmetric stretching mode of the solvent.

The deuteration of the hydroxyl group also increases relaxation rates. For all three isotope labeled thiocyanates, the T_1 relaxation rates in CH_3OD are similar and they are all faster

than in CH_3OH. In the case of $SeCN^-$ (result not shown), we also observed that CN stretch relaxation rate in CH_3OD was approximately twice faster (~19 ps) than in CH_3OH (~40 ps, see Table 2). Since both OH and OD stretching mode are much higher than the CN stretching mode frequency, the effect of hydrogen/deuterium substitution must result from the change in low-frequency modes. Two methanol modes below the CN stretch frequency undergo substantial change upon hydrogen/deuterium substitution: δ(COY) and δ(OY···O) where Y = H or D.[43] These modes are centered at ~940 and ~500 cm^{-1} in CH_3OD, and ~1420 and 670 cm^{-1} in CH_3OH. Our results suggest that these low-frequency modes in CH_3OD play an important role in assisting the vibrational relaxation of CN stretch.

Discussion

Relaxation Pathways. For polyatomic molecules in solution, there are two pathways for vibrational relaxation: direct intermolecular energy transfer (IET) and solvent-assisted IVR.[6,9,44,45] In the direct intermolecular vibrational energy transfer from solute to solvent molecules, the energy of CN stretch is transferred directly into solvent modes. For solvent-assisted IVR, the vibrational energy in the solute CN stretch mode is redistributed into other lower frequency modes of the solute and solvent molecules. This process can be expressed in the form of eq 2,

$$\hbar\Omega_{CN} = k\hbar\omega_{CX} + n\hbar\omega_{bend} + m\hbar\omega_{solvent} \qquad (2)$$

where ω_{CX} and ω_{bend} are intramolecular modes of XCN^-, $\omega_{solvent}$ is the low-frequency mode of solvent, and k, n, and m are quanta of corresponding modes. Thus, eq 2 describes the process on annihilation of one quanta of high-frequency CN stretch mode along with creation of k and n quanta of low-frequency modes of XCN^- and m solvent phonons. We define the order of the IVR process by the number of intramolecular vibration quanta exchanged in the process; that is, $(1 + k + n)$.[22,46] It has been demonstrated that the presence of the low-frequency modes of solvent accelerates the intramolecular vibrational relaxation of the high-frequency mode of solute molecules by enabling better energy matching.[22,45,47] Depending on the spectral density of the intramolecular states of solute, one can recognize two limiting mechanisms of IVR: statistical and state specific.[22] Since there are only a few intramolecular states below the (001) state of XCN^- anions, it is reasonable to expect that IVR processes are state specific.

For neutral polyatomic molecules in solution, the relaxation of a high-frequency mode (such as CH stretch, OH stretch) is often found to proceed through solvent assisted intramolecular vibrational relaxation (IVR).[5,7,9,22−26] For polar triatomic molecular in strongly interacting solvents such as HOD in D_2O, the vibrational relaxation of OH stretch also proceeds by solvent assisted IVR.[21] The mechanism for the vibrational relaxation of the asymmetric stretch mode of N_3^- in water is quite different; it involves both solvent assisted IVR and direct energy transfer to solvent molecules.[19]

We suggest that both solvent assisted IVR and direct energy transfer to solvent are involved in the vibrational relaxation of the CN stretching mode of the pseudo-halide anions studied in this work. The vibrational relaxation rate of the CN stretching mode of all XCN^- anions in H_2O and D_2O are significantly faster than those of diatomic molecule CN^- (28 ps in H_2O and 70 ps in D_2O),[15] despite their similar frequency. The rates are more similar to those of triatomic molecule N_3^- (1.2 ps in H_2O and 2.4 ps in D_2O).[27] It appears the availability of IVR pathways in charged polytomic molecules is responsible, at least in part, to the increase in the relaxation rate of high-frequency modes. There is also direct evidence for the solvent assisted IVR and direct solute to solvent energy transfer pathways. For example, the faster CN stretch relaxation rate of SCN^- in CH_3OD than in CH_3OH suggests the involvement of low frequency solvent modes, δ(COY) and/or δ(OY···O) (Y = D and H), in the solvent assisted IVR process. On the other hand, for $S^{12}C^{14}N^-$, $S^{12}C^{15}N^-$, and $S^{13}C^{14}N^-$, the relaxation rate of the CN stretching mode was found to increase as the CN stretch frequency became more in resonance with the CD_3 symmetric stretching band, as shown in Figure 6, but similar frequency dependence was not observed in CH_3OH, in which the CH_3 stretching band is far from resonance. This result suggests a direct energy transfer pathway to the CD_3 symmetric mode in CD_3OH. The T_1 relaxation time is faster in H_2O than in D_2O for all XCN^-, consistent with the better resonance of the CN stretching frequency with the solvent combination band in H_2O. However, comparison of relaxation rates in a series of SCN^- isotopes show that the relaxation rate does not show a clear correlation with solvent absorption in H_2O or D_2O, suggesting that direct IET is not the only relaxation pathway. These results suggest that both the direct IET and solvent assisted IVR pathways are present in these systems. However, their relative importance likely varies among the solutes and in different solvents.

Solute Dependence. In each of the investigated solvents the rate of vibrational relaxation increases in the series $SeCN^- < SCN^- < OCN^-$. Since the CN stretching mode frequencies are similar in these anions, the difference in the relaxation rates likely results from the changes in solvent−solute interaction strength and IVR pathways.

Going from X = O, S to Se, the partial charges on the X(−), C(+), and N(−) atoms become smaller.[34−36] Analysis of the spectral characteristics of the transient spectra reveals that the CN stretch bands of XCN^- anions are slightly red shifted and their bandwidths are about a factor of 2 narrower in DMSO and acetonitrile than the ones in the protic solvents. Both of these spectral changes were attributed to the formation of several (at least three in methanol) types of solute−solvent hydrogen-bonded species in protic solutions with solvent hydrogen-bonding to nitrogen and chalcogen atoms.[34−36] The increasing strength of the solute−solvent interaction in these series of solutes, resulted from higher partial charges in going from Se to O in XCN^- molecules, should enhance the rate of CN stretching mode relaxation in both the IET and solvent assisted IVR pathways. The effects of static Coulombic interaction and charge fluctuation in increasing the IET and IVR rates have been demonstrated in previous experimental and theoretical studies of polar molecules, such as I_2^-,[10,11] HgI,[12,13] CN^-,[14,15,18] N_3^-[1−9,27,29−31] and CH_3Cl,[16,17] in polar solvents.

Another major difference among XCN^- molecules is the frequencies of the CX stretch and bending modes, which decrease with the increase of the mass of the X atom (from X = O, S to Se), as shown in Table 1. The CX stretching frequency changes from 560 cm^{-1} in $SeCN^-$ to 1310 cm^{-1} in OCN^-. This large frequency change is expected have significant impact on the rates and pathways of IVR process. In general, the coupling strength for the different IVR pathways decreases with the order the process. If we limit our consideration to the fourth order or lower intramolecular coupling pathways, there are only a few energetically available intramolecular vibrational states below the initially excited CN stretch mode (001). They are shown in the upper row of Table 4. The energies of these states are

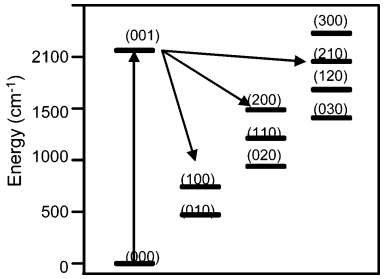

Figure 7. An energy diagram of intramolecular vibrational states of SCN^- and possible solvent assisted vibrational relaxations paths (horizontal arrows) from initially excited (001) state (see also Table 4). The IVR accepting states are shown on the right of (001) and grouped into columns according to their coupling order.

TABLE 4: Frequency Mismatch between Initially Excited CN Stretch (001) State and Intramolecular Vibrational States (IVR) of XCN^-

IVR states →	(100)	(010)	(110)	(200)	(020)	(210)	(120)	(300)	(030)
OCN^-	858	1536	226	−452	904	−1084	−406	−1762	272
SCN^-	1320	1593	850	577	1123	107	380	−166	653
$SeCN^-$	1513	1653	1093	953	1233	533	673	394	814

estimated using harmonic frequencies. The energy mismatch between initial state and IVR states are also shown in Table 4. Shown in Figure 7 is a schematic diagram of the initial states and the possible IVR states for SCN^- molecules. If we further assume that interaction with the solvent does not change the symmetry of the molecule and intramolecular anharmonicity is crucial for the solvent assisted IVR process, then the number of relaxation pathways can be further reduced by considering the symmetry of the states.[19]

In all these pathways, there exist large energy mismatches between the (001) state and final IVR states, and participation of solvent modes is needed. For the same IVR pathways, the energy mismatch increases in the XCN^- series from X = O to S and Se, because of a decrease in the frequency of CX stretching and bending modes. According to the Landau−Teller formula, the rate of solvent assisted IVR depends on the strength of the coupling matrix element between the initial and final states and the spectral density of the solvent friction force at the mismatch frequency.[2,19,21] The former depends on the intramolecular anharmonic potential and the interaction with the solvent. In general, the power spectrum of the solvent friction force on solute vibrational modes decreases rapidly (nearly exponentially) with the frequency, except for resonances at the frequency of the solvent vibrational modes.[10,12,16−19,21] For example, in the computational study of the vibrational relaxation of the OH stretch mode of HOD in D_2O, it was found that the dominating relaxation pathway was via the overtone of the bending mode because of its smallest energy mismatch with the initial state (despite smaller coupling matrix elements than transition to the ground state).[21] It seems likely that both the increasing frequency mismatch and the decrease of partial charges can account for the trend of decreasing vibrational relaxation rates in XCN^- from X = O to S and Se in all solvents studied here. However, discerning the relative importance of these effects will require a more detailed computation study, similar to those that have been reported for other polyatomic molecules.[19,21]

Summary

We have measured the T_1 relaxation time of the CN stretch of XNC^- (X = O, S, Se) in H_2O, D_2O, CH_3OH, DMSO, and CH_3CN. The relaxation time of various SCN^- isotopes ($S^{12}C^{14}N^-$, $S^{13}C^{14}N^-$, $S^{12}C^{15}N^-$) in H_2O and D_2O and in deuterated methanols (CD_3OH, CD_3OD, CH_3OD, and CH_3OH) were also measured. In all the solvents studied, the relaxation rates follow the order of $OCN^- > SCN^- > SeCN^-$. This trend is attributed to stronger solvent−solvent interaction owing to larger partial charges on the X, C, and N atoms, and smaller frequency mismatch in IVR pathways in going from X = Se to S to O. For all three anions and the isotope of SCN^-, the relaxation rate is faster in H_2O than in D_2O and other solvents. For various SCN^- isotopes in deuterated methanols, we observed enhancement of the T_1 relaxation rate of the CN stretching mode in methanols with CD_3 groups, and the factor of enhancement depends on the degree of resonance of CN frequency with the CD_3 stretching band. We attribute this to direct energy transfer from the CN stretching to the CD_3 symmetric stretching mode. We also observed that the relaxation rate in CH_3OD is faster than in CH_3OH, suggesting solvent assisted IVR pathways that involve low frequency solvent modes in CH_3OD.

While there is experimental evidence for both the direct IET and solvent assisted IVR processes, the relative contribution of these pathways in different anions/solvent system is unclear. To provide more information on the relaxation pathways, additional experiments that can directly probe the low-frequency modes, such as two color IR pump−probe and/or IR pump−anti-Stokes Raman probe, are needed.[9] More importantly, a detailed understanding of the relaxation mechanism would likely require a computational study that includes both IET and IVR pathways and takes into account solute partial charge and polarization.[19]

Acknowledgment. The work is supported by the National Science Foundation through Grant CHE-0514662, the Emory University Research Committee, and in part by the donor of the Petroleum Research Fund. T.L. is an Alfred P. Sloan fellow.

References and Notes

(1) Laubereau, A.; Kaiser, W. *J. Mod. Phys.* **1978**, *50*, 607.
(2) Oxtoby, D. W. *Annu. Rev. Phys. Chem.* **1981**, *32*, 77.
(3) Heilweil, E. J.; Casassa, M. P.; Cavanagh, R. R.; Stephenson, J. C. *Annu. Rev. Phys. Chem.* **1989**, *40*, 143.
(4) Harris, C. B.; Smith, D. E.; Russell, D. J. *Chem. Rev.* **1990**, *90*, 481.
(5) Elsaesser, T.; Kaiser, W. *Annu. Rev. Phys. Chem.* **1991**, *42*, 83.
(6) Owrutsky, J. C.; Raftery, D.; Hochstrasser, R. M. *Annu. Rev. Phys. Chem.* **1994**, *45*, 519.
(7) Rey, R.; Moller, K. B.; Hynes, J. T. *Chem. Rev.* **2004**, *104*, 1915.
(8) Fujisaki, H.; Bu, L.; Straub, J. E. *Adv. Chem. Phys.* **2005**, *130*, 179.
(9) Dlott, D. D. *Chem. Phys.* **2001**, *266*, 149.
(10) Benjamin, I.; Barbara, P. F.; Gertner, B. J.; Hynes, J. T. *J. Phys. Chem.* **1995**, *99*, 7557.
(11) Walhout, P. K.; Alfano, J. C.; Thakur, K. A. M.; Barbara, P. F. *J. Phys. Chem.* **1995**, *99*, 7568.
(12) Gnanakaran, S.; Hochstrasser, R. M. *J. Chem. Phys.* **1996**, *105*, 3486.
(13) Pugliano, N.; Szarka, A. Z.; Gnanakaran, S.; Triechel, M.; Hochstrasser, R. M. *J. Chem. Phys.* **1995**, *103*, 6498.
(14) Heilweil, E. J.; Doany, F. E.; Moore, R.; Hochstrasser Robin, M. *J. Chem. Phys.* **1982**, *76*, 5632.
(15) Hamm, P.; Lim, M.; Hochstrasser, R. M. *J. Chem. Phys.* **1997**, *107*, 10523.
(16) Whitnell, R. M.; Wilson, K. R.; Hynes, J. T. *J. Chem. Phys.* **1992**, *96*, 5354.
(17) Whitnell, R. M.; Wilson, K. R.; Hynes, J. T. *J. Phys. Chem.* **1990**, *94*, 8625.
(18) Rey, R.; Hynes, J. T. *J. Chem. Phys.* **1998**, *108*, 142.
(19) Morita, A.; Kato, S. *J. Chem. Phys.* **1998**, *109*, 5511.
(20) Ladanyi, B. M.; Stratt, R. M. *J. Chem. Phys.* **1999**, *111*, 2008.
(21) Rey, R.; Hynes, J. T. *J. Chem. Phys.* **1996**, *104*, 2356.
(22) Elles, C. G.; Bingemann, D.; Heckscher, M. M.; Crim, F. F. *J. Chem. Phys.* **2003**, *118*, 5587.

(23) Elles, C. G.; Cox, M. J.; Crim, F. F. *J. Chem. Phys.* **2004**, *120*, 6973.
(24) Tokmakoff, A.; Sauter, B.; Fayer, M. D. *J. Chem. Phys.* **1994**, *100*, 9035.
(25) Iwaki, L. K.; Dlott, D. D. *J. Phys. Chem. A* **2000**, *104*, 9101.
(26) Seifert, G.; Zuerl, R.; Graener, H. *J. Phys. Chem. A* **1999**, *103*, 10749.
(27) Li, M.; Owrutsky, J.; Sarisky, M.; Culver, J. P.; Yodh, A.; Hochstrasser, R. M. *J. Chem. Phys.* **1993**, *98*, 5499.
(28) Zhong, Q.; Baronavski, A. P.; Owrutsky, J. C. *J. Chem. Phys.* **2003**, *119*, 9171.
(29) Owrutsky, J. C.; Kim, Y. R.; Li, M.; Sarisky, M. J.; Hochstrasser, R. M. *Chem. Phys. Lett.* **1991**, *184*, 368.
(30) Zhong, Q.; Owrutsky, J. C. *Chem. Phys. Lett.* **2004**, *383*, 176.
(31) Zhong, Q.; Baronavski, A. P.; Owrutsky, J. C. *J. Chem. Phys.* **2003**, *118*, 7074.
(32) Yarne, D. A.; Tuckerman, M. E.; Klein, M. L. *Chem. Phys.* **2000**, *258*, 163.
(33) Ferrario, M.; Klein, M. L.; McDonald, I. R. *Chem. Phys. Lett.* **1993**, *213*, 537.
(34) Schultz, P. W.; Leroi, G. E.; Harrison, J. F. *Mol. Phys.* **1996**, *88*, 217.
(35) Schultz, P. W.; Leroi, G. E.; Popov, A. I. *J. Am. Chem. Soc.* **1995**, *117*, 10735.
(36) Schultz, P. W.; Leroi, G. E.; Popov, A. I. *J. Am. Chem. Soc.* **1996**, *118*, 10617.
(37) Brooker, M. H.; Wen, N. P. *Can. J. Chem., Rev. Can. Chim.* **1993**, *71*, 1764.
(38) Jones, L. H. *J. Chem. Phys.* **1956**, *25*, 1069.
(39) Nakamoto, K. *Infrared and Raman Spectra of Inorganic and Coordination Coumpounds*, 3rd ed.; John Wiley & Sons: New York, 1978.
(40) Bachelin, M.; Gans, P.; Gill, J. B. *J. Chem. Soc., Faraday Trans.* **1992**, *88*, 3327.
(41) Bertie, J. E.; Ahmed, M. K.; Eysel, H. H. *J. Phys. Chem.* **1989**, *93*, 2210.
(42) Chabanel, M. *Pure Appl. Chem.* **1990**, *62*, 36.
(43) Bertie, J. E.; Zhang, S. L. L. *J. Mol. Struct.* **1997**, *413*, 333.
(44) Nitzan, A.; Mukamel, S.; Jortner, J. *J. Chem. Phys.* **1975**, *63*, 200.
(45) Kenkre, V. M.; Tokmakoff, A.; Fayer, M. D. *J. Chem. Phys.* **1994**, *101*, 10618.
(46) Gruebele, M. *Adv. Chem. Phys.* **2001**, *114*, 193.
(47) Stratt, R. M.; Maroncelli, M. *J. Phys. Chem.* **1996**, *100*, 12981.